

Long-term memory and delayed shear localisation in soft glassy materials

Henry A. Lockwood, Matthew P. Carrington and Suzanne M. Fielding

Department of Physics, Durham University, Science Laboratories, South Road, Durham DH1 3LE, UK

(Dated: July 15, 2019)

We study theoretically the dynamics of soft glassy materials during the process of stress relaxation following the rapid imposition of a shear strain. By detailed numerical simulations of a mesoscopic soft glassy rheology model and three different simplified continuum fluidity models, we show that a dramatic shear localisation instability arises, in which the strain field suddenly becomes heterogeneous within the sample, accompanied by a precipitous drop in the stress. Remarkably, this instability can arise at extremely long delay times after the strain was applied, due to the long-term memory inherent to glassy systems. The finding that a catastrophic mechanical instability can arise long after any deformation could have far reaching consequences for material processing and performance, and potentially also for delayed geophysical phenomena.

Many soft materials, including dense colloids, microgels, emulsions and foams, show notable shared features in their rheological (deformation and flow) properties. Their steady state flow curve of shear stress $\sigma(\dot{\gamma})$ as a function of shear rate $\dot{\gamma}$ shows a yield stress in the limit of slow flows, $\sigma_y = \lim_{\dot{\gamma} \rightarrow 0} \sigma(\dot{\gamma})$ [1]. The viscoelastic spectra $G^*(\omega)$ characterising their stress response to an imposed strain oscillation are typically rather flat functions of the oscillation frequency ω [2]. These shared rheological features indicate the presence of sluggish stress relaxation modes, and have been attributed to the underlying presence of the basic glassy features of disorder (e.g., in a disordered packing of emulsion droplets), and metastability (with large energy barriers impeding droplet rearrangements) [3]. Similarly amorphous, but harder materials include polymeric, metallic and structural glasses.

Following the switch-on of a shear flow in an initially well rested sample, such a material will typically respond initially elastically, before plastically yielding into a finally fluidised state [1]. Commonly observed during this process of yielding is the phenomenon of *shear localisation*: a state of initially homogeneous shear in the elastic regime gives way during plastic yielding to the formation of shear bands [4–16]: layers of differing viscosity that coexist within the material. These bands may eventually heal to leave a homogeneously fluidised flowing state. In harder materials, shear localisation more often results in catastrophic material failure [17]. In geophysics, it is implicated in earthquakes, landslides and mudslips [18, 19].

Besides sustained deformations of the kind just described, in which (given a constant imposed shear rate $\dot{\gamma}$) the shear strain $\gamma = \dot{\gamma}t$ accumulates indefinitely over time t and the material yields into a steadily flowing state, another commonly imposed type of deformation involves instead simply straining a material by a finite amount, which we shall denote γ_0 in what follows. The strain is held constant thereafter, with no further deformation applied. This will be modelled below by a step function, $\gamma(t) = \gamma_0\Theta(t - t_w)$, though the physics we present holds for any reasonably short time interval of deformation. We denote the time of strain application $t = t_w$, defined relative to the sample having been freshly prepared at an earlier time $t = 0$. The shear stress initially generated

by this deformation, $\sigma(t = t_w^+)$, then typically decays as a function of the subsequent time interval $\Delta t = t - t_w$, with the material slowly relaxing towards a stress-free, quiescent state as $\Delta t \rightarrow \infty$. Widely observed in soft glassy materials is the phenomenon of *ageing*, in which a significant part of this stress relaxation takes place on timescales that grow with the sample age t_w [20–27]: a property that has been termed ‘long-term memory’ [28].

Given the absence in such a scenario of any finally flowing state, it has been widely assumed that this post-strain stress relaxation will take place in a straightforwardly innocuous way, with the material simply slowly returning to a homogeneous relaxed state. This Letter will show, on the contrary, that for a wide range of values of amplitude γ_0 and time t_w of imposed strain, the material will instead suffer a catastrophic internal instability in which it suddenly becomes highly heterogeneous within itself, accompanied by a precipitous drop in the stress. We further show that this instability can be delayed long into the process of stress relaxation, with the delay time Δt^* increasing linearly with the initial sample age t_w . Remarkably, therefore, the delay time can become arbitrarily large for old systems, $t_w \rightarrow \infty$. An observer lacking any knowledge of the long historic deformation could thus be caught entirely unawares by the instability.

We shall demonstrate this phenomenon by detailed numerical simulations of a mesoscopic soft glassy rheology model [3]. We show it also to hold in a three different variants of a highly simplified continuum fluidity model [12]. In thus confirming it to be independent of the particular constitutive model used, we suggest it may be generic across amorphous materials, with far reaching consequences for material processing and performance, and potentially also for delayed geophysical phenomena such as mudslips and seismic aftershocks.

Throughout we assume incompressible, inertialess deformations in which the displacement, velocity and stress fields within the material, $\mathbf{u}(\mathbf{r}, t)$, $\mathbf{v}(\mathbf{r}, t)$ and $\boldsymbol{\Sigma}(\mathbf{r}, t)$, obey the standard conditions of mass balance, $\nabla \cdot \mathbf{u} = 0$ and $\nabla \cdot \mathbf{v} = 0$, and of force balance, $\nabla \cdot \boldsymbol{\Sigma} = 0$. The total stress $\boldsymbol{\Sigma} = \boldsymbol{\sigma} + 2\eta\mathbf{D} - p\mathbf{I}$ in any fluid element is assumed to comprise an elastoplastic contribution $\boldsymbol{\sigma}$ from the mesoscopic substructures (emulsions droplets, micro-

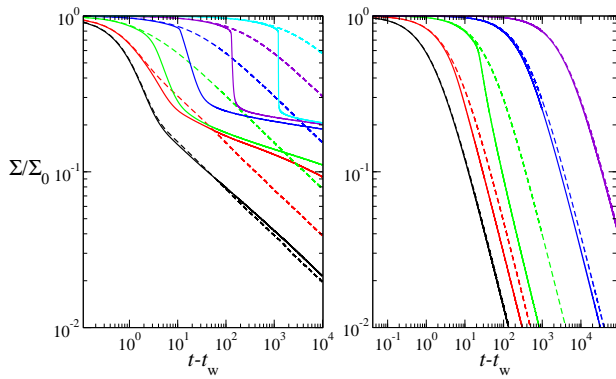


FIG. 1. Stress decay as a function of the time interval $\Delta t = t - t_w$ since the imposition of a step shear strain. **Left:** SGR model at a noise temperature $x = 0.3$ for a strain amplitude $\gamma_0 = 2.5$ and waiting times $t_w = 10^3, 10^4, \dots, 10^8$ in curves left to right. **Right:** fluidity model for $\gamma_0 = 5.5$ and waiting times $t_w = 10^4, 10^5, 10^6, 10^7, 10^8$ in curves left to right. Dashed curves show the results of calculations in which the strain field is artificially constrained to remain homogeneous, and solid lines in which it is allowed to become heterogeneous.

gel beads, etc), a Newtonian solvent contribution of viscosity η , and an isotropic pressure, p . Here $K_{\alpha\beta} = \partial_\beta v_\alpha$ and $\mathbf{D} = \frac{1}{2}(\mathbf{K} + \mathbf{K}^T)$. In considering only imposed displacements of the (initial) form $\mathbf{u}(\mathbf{r}, t) = u(y)\hat{\mathbf{x}} = \gamma_0 y \hat{\mathbf{x}}$, we restrict all displacements and velocities to the direction $\hat{\mathbf{x}}$ and all gradients to the direction $\hat{\mathbf{y}}$. Relevant associated fields are then the displacement $u(y, t)$, strain $\gamma(y, t) = \partial_y u(y, t)$, velocity $v(y, t) = \dot{u}(y, t)$ and strain-rate $\dot{\gamma}(y, t) = \partial_y v(y, t)$. For the dynamics of the elastoplastic stress $\boldsymbol{\sigma}$ we shall use two different constitutive models. As suited to deformations of the form just described, we track only the shear stress components σ_{xy} and $\Sigma_{xy} = \sigma_{xy} + \eta\dot{\gamma}$ of the viscoelastic and total stresses, further dropping the xy subscript for clarity.

The first constitutive model to be used is the soft glassy rheology (SGR) model [3]. This considers an ensemble of elements, each corresponding to a local mesoscopic region of material (a few tens of emulsion droplets, say). Under an imposed shear deformation of rate $\dot{\gamma}$, each element experiences a buildup of local elastic shear strain l according to $\dot{l} = \dot{\gamma}$, with a corresponding stress Gl , given a constant modulus G . This is intermittently released by local plastic yielding events, each of which is modelled as hopping of an element over a strain-modulated energy barrier E , governed by a noise temperature x , with the yielding intervals chosen stochastically with rate $\tau_0^{-1} \exp[-(E - \frac{1}{2}kl^2)/x]$. Upon yielding, any element resets its local stress to zero and selects its new energy barrier at random from an exponential distribution $\exp(-E/x_g)$. This confers a broad spectrum of yielding times, $P(\tau)$. It also results in a glass phase for $x < x_g$, in which, in the absence of flow, a material shows rheological ageing: the timescale for the relaxation of the macroscopic stress $\langle Gl \rangle$ follows a step strain increases lin-

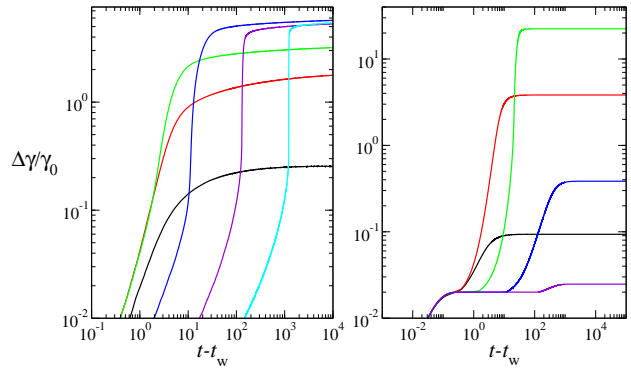


FIG. 2. Degree of strain heterogeneity $\Delta\gamma$ across the sample, normalised by the imposed strain γ_0 , as a function of the time interval $\Delta t = t - t_w$ since the imposition of a step shear strain, for a fixed strain amplitude γ_0 and waiting times t_w as in Fig. 1. **Left:** SGR model. **Right:** fluidity model.

early with the sample age t_w . A steadily imposed shear flow however interrupts ageing, and the steady state flow curve has a yield stress. Full details of the SGR model in its original, spatially uniform form are in Ref. [3].

The model's adaptation to account for non-uniform deformations is discussed in [12, 29]. This involves numerically taking $m = 1 \dots M$ SGR elements on each of $n = 1 \dots N$ streamlines at discretised flow-gradient positions $y = 0 \dots L_y$, with periodic boundary conditions. The viscoelastic stress on streamline n is $\sigma_n = (G/M) \sum_m l_{nm}$. Given an imposed average shear rate $\bar{\dot{\gamma}}$ across the sample as a whole (which in our case is zero at all times apart from t_w), the shear rate on each streamline n is then calculated, by enforcing force balance, to be $\dot{\gamma}_n = \bar{\dot{\gamma}} + (\bar{\sigma} - \sigma_n)/\eta$, where $\bar{\sigma} = (1/N) \sum_n \sigma_n$.

Our second model is a highly simplified continuum fluidity model [12], which supposes a Maxwell-type constitutive equation for the viscoelastic stress

$$\partial_t \sigma(y, t) = G\dot{\gamma} - \sigma/\tau, \quad (1)$$

where G is a constant modulus and τ is a structural relaxation time (inverse fluidity) that has its own dynamics:

$$\partial_t \tau = f(\tau, \sigma, \dot{\gamma}) + l_o^2 \partial_y^2 \tau. \quad (2)$$

We have considered three different model variants within this general form. The first has $f = 1 - |\dot{\gamma}|(\tau - \tau_0)(|\sigma| - \sigma_{th})\Theta(|\sigma| - \sigma_{th})$ with $\sigma_{th} = 1$; the second has $f = 1 - |\dot{\gamma}|(\tau - \tau_0)$; the third has $f = 1 - \tau/(\tau_0 + 1/|\dot{\gamma}|)$. Each captures rheological ageing, with the timescale for stress relaxation following the imposition of a step strain increasing linearly with the system age, $\tau = t_w$. A steady flow cuts off ageing at the inverse strain rate, and the steady state flow curve displays a yield stress. The results that we present below are all obtained within the first functional form for f , but we have checked that the same scenario qualitatively holds within all three variants. The parameter l_o in Eqn. 2 is a mesoscopic length

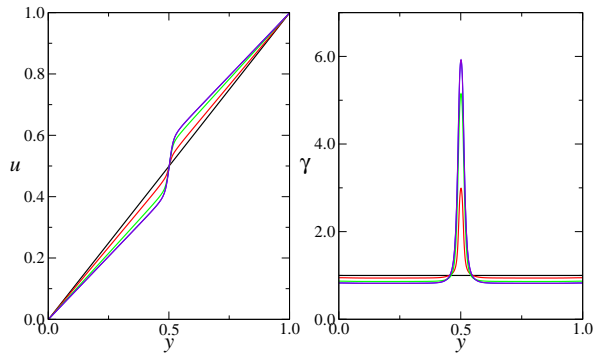


FIG. 3. **Left:** displacement as a function of position across the sample at time intervals $\Delta t = 0.0$ (black), 40.0 (red), 45.0 (green), 60.0 (blue) and 80.0 (violet) following the imposition of a strain of amplitude $\gamma_0 = 7.0$ at a waiting time $t_w = 10^{10}$ in the fluidity model. **Right:** corresponding strain field. Profiles for $\Delta t = 60.0$ and 80.0 are indistinguishable.

describing the tendency for the relaxation time of a mesoscopic region to equalise with those of its neighbours.

Within each of these constitutive models, we shall consider a slab of material sandwiched between infinite flat parallel plates at $y = 0, L_y$. We assume it to be freshly prepared at time $t = 0$ in a fully rejuvenated initial state with zero stress across the whole sample, $\sigma(y, t = 0) = 0$. The sample is then left to age undisturbed until a time t_w , when it is suddenly subject to an (initially) uniform shear deformation $\mathbf{u}(\mathbf{r}, t) = \gamma_0 y \hat{\mathbf{x}}$, by displacing the top plate relative to the bottom one a distance $\gamma_0 L_y$ in the positive $\hat{\mathbf{x}}$ direction, generating a stress $\sigma(t = t_w^+) = G\gamma_0$. (In reality, inertia requires a non-zero time to accomplish this; as noted above, the scenario we present holds for any short deformation interval.) No further (global) strain is imposed thereafter, with zero average shear rate across the sample $\bar{\dot{\gamma}} \equiv \int_0^{L_y} \dot{\gamma}(y, t) dy = 0$.

As a function of the subsequent time $\Delta t = t - t_w$, we track the decay back to zero of the (total) shear stress $\Sigma(\Delta t)$. We also track the displacement field $u(y, \Delta t)$ and associated strain field $\gamma(y, \Delta t) = \partial_y u(y, \Delta t)$ within the sample. Note that the (initially uniform) strain field $\gamma(y, \Delta t)$ can become heterogeneous across the sample (y -dependent) as a result of the instability that we report, whereas Σ must remain uniform by force balance. To seed the instability, we add a small initial heterogeneity across the sample. We have checked that the scenario we present is robust to the nature and size of this.

We rescale strain, stress, time and length so that $x_g = G = \tau_0 = L_y = 1$. The solvent viscosity η is expected to be much less than the viscosity scale of the viscoelastic component, $G\tau_0 = 1$, but is otherwise unimportant to the physics we describe. For simplicity we set $\eta = 0.05$, but have checked for robustness in variations in this.

Fig. 1 shows the stress decay in the SGR model (left), and fluidity model (right), following the imposition of a step strain of a fixed amplitude, γ_0 , for several different

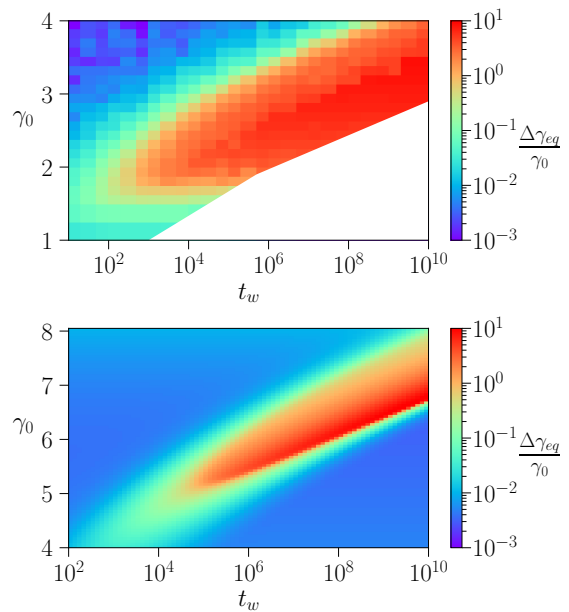


FIG. 4. Colourmap showing the normalised degree of strain heterogeneity $\Delta\gamma/\gamma_0$ attained at long times after the imposition of a step strain as a function of the amplitude γ_0 of the imposed strain and the sample age t_w at the time the strain was applied. **Top:** in the SGR model at $x = 0.3$. In the region shown in white, run-times are too long to obtain results across a full phase diagram, although slices (of the time at which the instability occurs) are shown to $t_w = 10^{10}$ for several γ_0 in Fig. 5. **Bottom:** in the fluidity model.

sample ages t_w . In each case, the timescale of stress decay increases with the sample age at the time the strain is imposed. The dashed lines show the results of calculations in which the strain field $\gamma(y)$ is artificially constrained to remain homogeneous during the stress decay, independent of y . The solid lines show calculations in which it is allowed to become heterogeneous across the sample. The departure of the latter from the former marks the onset of an instability in which the strain field becomes heterogeneous, accompanied by a more precipitous drop in the stress signal than is predicted by the artificially constrained homogeneous calculation.

To characterise the degree of growing heterogeneity, we define the quantity $\Delta\gamma(\Delta t)$ as the difference at any time Δt post-strain between the maximum of the strain $\gamma(y, \Delta t)$ across the flow gradient direction y , and the correspondingly defined minimum strain. The time-evolution of this quantity is shown in Fig. 2, with parameter values and line colours corresponding to those of the stress decay in Fig. 1. The divergence of the stress decay curves between the (enforced to be) homogeneous and (allowed to be) heterogeneous runs in Fig. 1 indeed arises contemporarily with the formation of a heterogeneous strain field, as characterised by the growth of $\Delta\gamma(t)$ in Fig. 2. At long times the strain heterogeneity settles to a constant in the fluidity model. (In the SGR model, it continues a very slow logarithmic growth due to the small

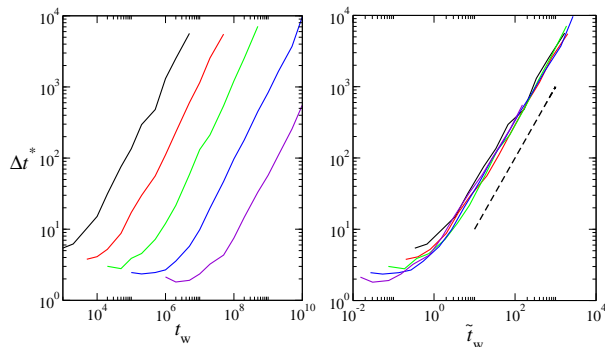


FIG. 5. **Left:** time interval Δt^* following the imposition of a step strain at which the strain localisation instability arises, as calculated within the SGR model. Results are plotted as a function of the sample age t_w at the time the strain is imposed, for different values of the strain amplitude: $\gamma_0 = 2.0, 2.25, 2.5, 2.75, 3.0$ in curves left to right. **Right:** same data replotted as a function of the scaled time $\tilde{t}_w = t_w \exp(-\alpha\gamma_0^2/2x)$ with $\alpha \approx 1.2$. Dashed line shows $\Delta t^* = \tilde{t}_w$ as a guide to the eye.

noise present our stochastic simulations, which however decreases with increasing number of elements M .)

For one particular value of imposed strain amplitude γ_0 and waiting time t_w , we show in Fig. 3 the displacement field $u(y, \Delta t)$ and the strain field $\gamma(y, \Delta t)$, at several time intervals Δt following the imposition of the strain, as calculated within the fluidity model. As can be seen, the initially linear displacement field $u(y, \Delta t = 0) = \gamma_0 y$ gives way to a non-linear one, associated with a pronounced heterogeneity in the strain field $\gamma(y, \Delta t)$, consistent with the observed temporal growth in $\Delta\gamma(\Delta t)$. The same quantities computed in the SGR model display the same behaviour (not shown).

We discussed in Fig. 2 the growth in strain heterogeneity $\Delta\gamma(\Delta t)$ as a function of the time Δt post-strain, for one fixed value of the imposed strain amplitude γ_0 and several values of the sample age t_w . In Fig. 4, we summarise in a ‘phase diagram’ colourmap the limiting degree of strain heterogeneity $\Delta\gamma$ at long times in the full plane of γ_0, t_w . (In practice, we take this value at the final time of the run for the fluidity model, and just after the precipitous rise in this quantity in the SGR model, to cutoff the slow logarithmic growth still present at long times in the SGR model.) Each coordinate pair (γ_0, t_w) in this plane corresponds to a single step strain experiment, with the colour scale showing the final degree of strain heterogeneity, normalised by the amplitude of the initially imposed strain: $\Delta\gamma/\gamma_0$. A significant degree of strain heterogeneity is observed across large regions of this parameter space, in both the SGR model (top) and fluidity model (bottom). In the region shown as white for the SGR model, run times are too long to obtain results.

We discuss finally the time delay Δt^* after the imposition of the strain at which the instability arises. We plot this in Fig. 5 (left) as a function of the sample age t_w for several values of the imposed strain amplitude γ_0 , in the SGR model. The same data are replotted in the right panel as a function of the scaled time $\tilde{t}_w = t_w \exp(-\alpha\gamma_0^2/2x)$, showing good data collapse onto a line $\Delta t^* \propto \tilde{t}_w$. The time at which the instability sets in can therefore be delayed long into the process of stress relaxation, with the delay time becoming arbitrarily long for initially old samples $t_w \rightarrow \infty$. It is worth emphasising this remarkable finding: that a catastrophic instability can arise within a material at indefinitely long times after any external deformation was last applied.

A banding instability after a rapid shear strain has been observed previously in polymer melts [30, 31], although after a short delay time of just a few seconds (consistent with the absence of long-term memory in those ergodic fluids), and having its origin in a non-monotonic relationship between stress and strain during the initial rapid straining process [32, 33]. No such non-monotonicity exists in any model explored here for an infinite rate of strain imposition, suggesting a fundamentally different instability mechanism in these soft glassy materials. Indeed, we suggest the mechanism to be as follows. Imagine an initially near uniform sample, but with a streamline (or region) in which the strain increases slightly relative to the rest of the sample. This slightly fluidises the material on that streamline, causing the elastoplastic stress σ to relax slightly faster. To maintain a uniform total stress Σ , that streamline must strain forward slightly further. This represents a positive feedback loop, leading to a runaway instability.

To summarise, we have uncovered a strain localisation instability that arises at long times after the imposition of a step strain in soft glassy materials, accompanied by a precipitous drop in the shear stress. We have explored the phenomenology of this instability via detailed numerical simulations of a mesoscopic soft glassy rheology model, and three different variants of a highly simplified continuum fluidity model. In finding the basic features to be the same across these different constitutive models, we suggest that the instability reported here may be generic across amorphous, glassy materials. We hope that these predictions will stimulate experimental studies aimed at observing this instability. A particularly remarkable feature is that the instability can arise at extremely long times after the initial strain imposition, i.e., long after the material last suffered any mechanical deformation, due to the long-term memory inherent to glassy materials. This could have far reaching consequences for material processing and performance, and for delayed geophysical phenomena such as seismic aftershocks.

- [2] D. Vlassopoulos and M. Cloitre, *Current opinion in colloid & interface science* **19**, 561 (2014).
- [3] P. Sollich, F. Lequeux, P. Hébraud, and M. E. Cates, *Physical review letters* **78**, 2020 (1997).
- [4] T. Divoux, D. Tamarii, C. Barentin, and S. Manneville, *Physical review letters* **104**, 208301 (2010).
- [5] J. D. Martin and Y. T. Hu, *Soft Matter* **8**, 6940 (2012).
- [6] T. Gibaud, C. Barentin, and S. Manneville, *Physical Review Letters* **101**, 258302 (2008).
- [7] C. J. Dimitriou and G. H. McKinley, *Soft Matter* **10**, 6619 (2014).
- [8] J. Colombo and E. Del Gado, *Journal of rheology* **58**, 1089 (2014).
- [9] Y. Shi, M. B. Katz, H. Li, and M. L. Falk, *Physical review letters* **98**, 185505 (2007).
- [10] G. P. Shrivastav, P. Chaudhuri, and J. Horbach, *Journal of Rheology* **60**, 835 (2016).
- [11] S. M. Fielding, *Reports on Progress in Physics* **77**, 102601 (2014).
- [12] R. L. Moorcroft, M. E. Cates, and S. M. Fielding, *Physical review letters* **106**, 055502 (2011).
- [13] M. L. Manning, J. S. Langer, and J. Carlson, *Physical review E* **76**, 056106 (2007).
- [14] M. Manning, E. Daub, J. Langer, and J. Carlson, *Physical Review E* **79**, 016110 (2009).
- [15] A. R. Hinkle and M. L. Falk, *Journal of Rheology* **60**, 873 (2016).
- [16] E. Jagla, *Journal of Statistical Mechanics: Theory and Experiment* **2010**, P12025 (2010).
- [17] M. J. Doyle, A. Maranci, E. Orowan, and S. Stork, *Proceedings of the Royal Society of London. A. Mathematical and Physical Sciences* **329**, 137 (1972).
- [18] E. G. Daub, M. L. Manning, and J. M. Carlson, *Journal of Geophysical Research: Solid Earth* **115** (2010).
- [19] P. Coussot, Q. D. Nguyen, H. Huynh, and D. Bonn, *Physical review letters* **88**, 175501 (2002).
- [20] K. Suman and Y. M. Joshi, *Langmuir* **34**, 13079 (2018).
- [21] M. Kaushal and Y. M. Joshi, *Soft Matter* **10**, 1891 (2014).
- [22] S. Rogers, P. Callaghan, G. Petekidis, and D. Vlassopoulos, *Journal of Rheology* **54**, 133 (2010).
- [23] L. Ramos and L. Cipelletti, *Physical review letters* **87**, 245503 (2001).
- [24] G. Yin and M. J. Solomon, *Journal of Rheology* **52**, 785 (2008).
- [25] C. Derec, G. Ducouret, A. Ajdari, and F. Lequeux, *Physical Review E* **67**, 061403 (2003).
- [26] C. Derec, A. Ajdari, G. Ducouret, and F. Lequeux, *Comptes Rendus de l'Académie des Sciences-Series IV-Physics* **1**, 1115 (2000).
- [27] S. M. Fielding, P. Sollich, and M. E. Cates, *Journal of Rheology* **44**, 323 (2000).
- [28] J.-P. Bouchaud, L. F. Cugliandolo, J. Kurchan, and M. Mezard, *Spin glasses and random fields*, 161 (1998).
- [29] S. Fielding, M. Cates, and P. Sollich, *Soft Matter* **5**, 2378 (2009).
- [30] P. E. Boukany, S.-Q. Wang, and X. Wang, *Macromolecules* **42**, 6261 (2009).
- [31] Y. Fang, G. Wang, N. Tian, X. Wang, X. Zhu, P. Lin, G. Ma, and L. Li, *Journal of Rheology* **55**, 939 (2011).
- [32] O. S. Agimelen and P. D. Olmsted, *Physical review letters* **110**, 204503 (2013).
- [33] R. L. Moorcroft and S. M. Fielding, *Journal of Rheology* **58**, 103 (2014).